

BOUNDARY MANIFOLDS FOR ENERGY SURFACES IN CELESTIAL MECHANICS*

ERNESTO A. LACOMBA**

*Departamento de Matemáticas, Universidad Autónoma Metropolitana-Iztapalapa, Apdo. Postal 55-534,
C.P. 09340, México 13, D.F., Mexico*

and

CARLES SIMÓ***

Facultat de Matemàtiques, Universitat de Barcelona, Gran Via, 585, Barcelona 7, Spain

Abstract. We complete Mc Gehee's picture of introducing a boundary (total collision) manifold to each energy surface. This is done by constructing the missing components of its boundary as other submanifolds, representing now the asymptotic behavior at infinity.

It is necessary to treat each case $h = 0$, $h > 0$ or $h < 0$ separately. In the first case, we repeat the known result that the behavior at total escape is the same as in total collision. In particular, we explain why the situation is radically different in the $h > 0$ case compared with the zero energy case. In the case $h < 0$ we have many infinity manifold components, and the general situation is not quite well understood.

Finally, our results for $h \geq 0$ are shown to be valid for general homogeneous potentials.

1. Introduction

The McGehee change of variables in Celestial Mechanics glues a boundary to each energy surface, as is well known. The goal of this paper is to construct the missing boundary components of the energy surfaces by adding other submanifolds representing the asymptotic behavior in escape motions. The novel idea is to blow up the infinity.

We will re-derive known results about escape orbits. In some examples we also illustrate the existence of some collision-escape orbits in the zero energy case.

Recall that in Celestial Mechanics one deals with a system of ordinary differential equations as

$$\begin{aligned}\dot{\mathbf{q}} &= \mathbf{p}A^{-1} \\ \dot{\mathbf{p}} &= \text{grad } U(\mathbf{q})\end{aligned}\tag{1}$$

where $\mathbf{p} \in \mathbb{R}^k$, $\mathbf{q} \in \mathbb{R}^k - \Delta$ and U is an analytic function homogeneous of degree -1 on \mathbb{R}^k , except for the subset $\Delta \subset \mathbb{R}^k$, where it is singular. The A is an order k constant matrix, called the mass matrix. This is a Hamiltonian system, whose Hamiltonian function is the total energy $H(\mathbf{q}, \mathbf{p}) = \frac{1}{2}\mathbf{p}A^{-1}\mathbf{p}^t - U(\mathbf{q})$. As is known, to any fixed energy surface $E_h = \{H = h\}$, McGehee's blow up of the origin [5] glues a codimension one-boundary submanifold, the total collision manifold. Moreover, the flow extends to a

* Paper presented at the 1981 Oberwolfach Conference on Mathematical Methods in Celestial Mechanics.

** The research conducted in this paper has been partially supported by CONACYT (México), under grant PCCBNAL 790178.

*** Partially supported by an Ajut a l'Investigació of the University of Barcelona.

fictitious flow on the boundary, which gives important information about motions close to total collision.

In order to add the boundary components of E_h corresponding to the asymptotic behavior of escape to infinity, we have to consider three different cases for the energy values $h \in \mathbb{R}$.

2. Zero Energy Surfaces

The idea is to generalize McGehee's change of variables by now blowing up the infinity in configuration space in the same way as he did with the origin. For that, we rather take as scaling variable $\rho = I^{-1/2}$, where $I = \mathbf{q}A\mathbf{q}'$ is the moment of inertia. We then make for $h = 0$ the change of variables $\mathbf{Q} = \rho\mathbf{q}$, $\mathbf{P} = \rho^{-1/2}\mathbf{p}$. Then the system of differential Equations (1) becomes

$$\begin{aligned}\dot{\rho} &= -\rho^{5/2}v \\ \dot{\mathbf{Q}} &= -\rho^{3/2}v\mathbf{Q} + \rho^{3/2}\mathbf{P}A^{-1} \\ \dot{\mathbf{P}} &= \frac{1}{2}\rho^{3/2}v\mathbf{P} + \rho^{3/2}\text{grad } U(\mathbf{Q})\end{aligned}\tag{2}$$

with the notation $v = \mathbf{P} \cdot \mathbf{Q}$, the normalization condition $\mathbf{Q}A\mathbf{Q}' = 1$, and the new energy relation

$$\mathbf{P}A^{-1}\mathbf{P}' = 2U(\mathbf{Q}) + 2h/\rho.\tag{3}$$

Notice that (3) is singular when $\rho = 0$, so that the transformation mentioned works only in our case $h = 0$. On the other hand, (2) is regular but annihilates at $\rho = 0$. We therefore, make a time-scaling $d\tau = \rho^{3/2}dt$, which eliminates the unpleasant factor $\rho^{3/2}$. We then get the following system, where $'$ denotes derivatives with respect to the new time τ

$$\begin{aligned}\rho' &= -\rho v \\ \mathbf{Q}' &= -v\mathbf{Q} + \mathbf{P}A^{-1} \\ \mathbf{P}' &= \frac{1}{2}v\mathbf{P} + \text{grad } U(\mathbf{Q}),\end{aligned}\tag{4}$$

with the constraint $\mathbf{Q}A\mathbf{Q}' = 1$.

We now notice that (4) almost equals Mc Gehee's system of differential equations [5]. We only have to substitute ρ by $r = \rho^{-1}$ in the scaling, and as a result the first equation in (4) will change sign.

For zero energy and n bodies, several authors have found the same asymptotic behavior at parabolic (total) escape as at total collision. Below we obtain a very simple proof and a topological interpretation of this statement.

We see that the set

$$N_0 = \{(\rho, \mathbf{Q}, \mathbf{P}) : \rho = 0, \quad \mathbf{Q}A\mathbf{Q}' = 1, \quad \mathbf{P}A^{-1}\mathbf{P}' = 2U(\mathbf{Q})\}$$

is invariant under the flow (4). We will call this the *infinity manifold*, and it indeed

appears as a boundary submanifold glued to the zero energy surface

$$E_0 = \{(\rho, \mathbf{Q}, \mathbf{P}) : \rho > 0, \quad \mathbf{Q}\mathbf{A}\mathbf{Q}^t = 1, \quad \mathbf{P}\mathbf{A}^{-1}\mathbf{P}^t = 2U(\mathbf{Q})\}.$$

In fact, analytically (and topologically, of course) it is the same as the total collision manifold C , except for the different meaning of the radial variable. Indeed,

$$C = \{(r, \mathbf{Q}, \mathbf{P}) : r = 0, \quad \mathbf{Q}\mathbf{A}\mathbf{Q}^t = 1, \quad \mathbf{P}\mathbf{A}^{-1}\mathbf{P}^t = 2U(\mathbf{Q})\}. \quad (5)$$

THEOREM 1. *If $h = 0$, the flow on N_0 is exactly the same as in the total collision manifold C . In particular its equilibrium points, defining asymptotic behavior at parabolic escape, are given by central configurations of the system.*

Proof. From the remark above about the flow (4), the equilibrium points on N_0 are the same as those on C , since we get

$$\rho = 0, \quad \mathbf{P}\mathbf{A}^{-1} = v\mathbf{Q}, \quad v\mathbf{P} = -2 \operatorname{grad} U(\mathbf{Q}).$$

We know they are associated to central configurations, and the homographic solutions will simply connect equilibrium points on C , with the corresponding ones on N_0 , as we will clarify in the examples below.

The flow on N_0 is actually the same as the flow on C , since $\rho = 0$ in (4) leaves out exactly the same equations as $r = 0$ in McGehee's case. Q.E.D.

COROLLARY. *The flow on N_0 is gradient – as it is with respect to v .*

Moreover, since the energy relation becomes independent of ρ once we set $h = 0$ in (3), we see that (4) can first be solved in the \mathbf{Q}, \mathbf{P} variables, and then for ρ . This means that the flow is projectable on C or N_0 . Once we know the flow on either one of those boundary components, the flow on E_0 is obtained by lifting the solution up in the radial direction. It is like a mirror image in terms of $\ln \rho$.

By rephrasing the result for C , we conclude that in any n -body problem, escape to infinity takes place asymptotically by an approach to central configurations, or by keeping close to lower order collisions (escape by the arms in the collinear or isosceles 3-body problems).

Example 1. Consider the planar isosceles 3-body problem for the $h = 0$ case, where double collisions are regularized. Recall that one is given two particles of masses equal to 1, and a third one of mass α . Initial conditions are given so that, at any time, the configuration is an isosceles triangle, as shown in Figure 1.

When double collisions are regularized, the topology of C and the nature of its flow are well known (see [6]). The topology and flow of N_0 , with regularization of double collisions, will be likewise, by Theorem 1. We then arrive at Figure 2, where the energy surface E_0 is contained in the space between N_0 and C , and the homographic solutions are shown as connections between the two components N_0 and C of the boundary.

Topologically, this is the space between two concentric spheres minus four rays

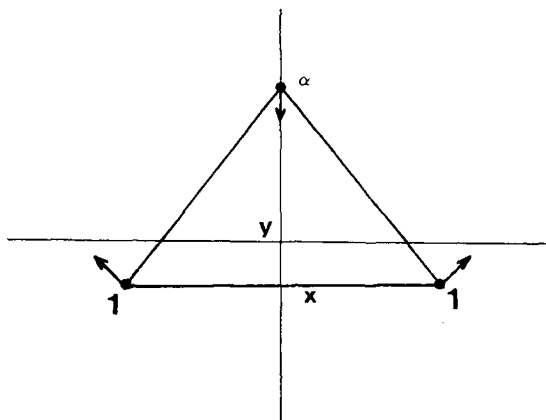


Fig. 1.

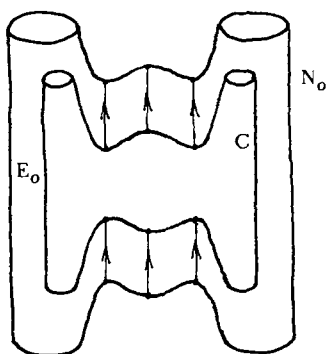
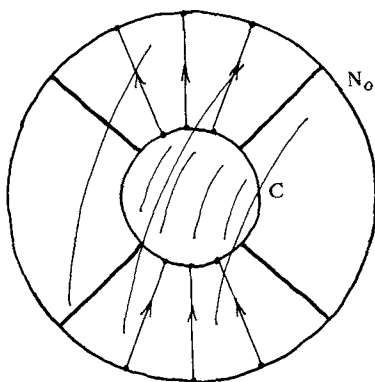


Fig. 2.

Fig. 3. Topological description of E_0 and its boundary surfaces N_0 , C .

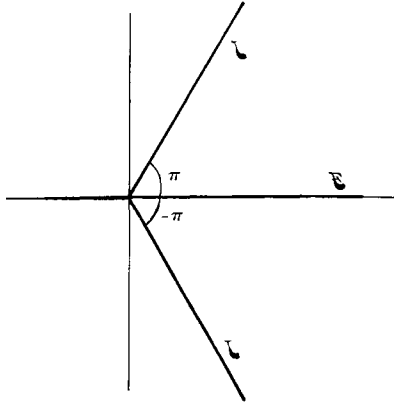


Fig. 4. Euler and Lagrange central configurations of the isosceles problem.

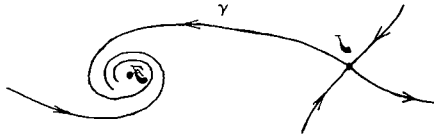


Fig. 5.

(due to the arms), as shown in Figure 3. This topology has already been described in [2], except that the boundary N_0 had not been taken into account. Somehow this way of looking at the topology cried out that something was missing.

In the configuration space of Jacobi coordinates in Figure 1, we see that central configurations correspond to the lines $\theta = 0, \theta = \pm \Pi/3$ in Figure 4.

We conclude that asymptotically the total escape to infinity is indeed by the above central configurations, or by $\theta = \pm \Pi/2$ (escape by the arms), and consider this a particular case of our general remark above.

Finally, knowledge about this projectable flow permits us to show the existence of some remarkable motions. By way of illustration, we will describe a motion starting as an ejection from a triple collision of an equilateral triangle type, and ending up in a total escape of a collinear type. This motion was shown to exist in [3] by a different method.

Recall that for the flow on C (or on N_0), Lagrange equilibrium points L are saddles. In the ejection (upper) part of C the Euler equilibrium point is a sink, with an orbit γ coming from the saddle, as Figure 5 shows in the spiraling case $\alpha < 55/4$.

The two ejecting orbits from the saddle are contained in the 2-dimensional invariant submanifold at L for the flow on $E_0 \cup C$. Therefore any orbit $\tilde{\gamma}$ on the above-mentioned invariant submanifold which projects into and is different from γ , will end up asymptotically in the corresponding Euler point of N_0 which projects over E .

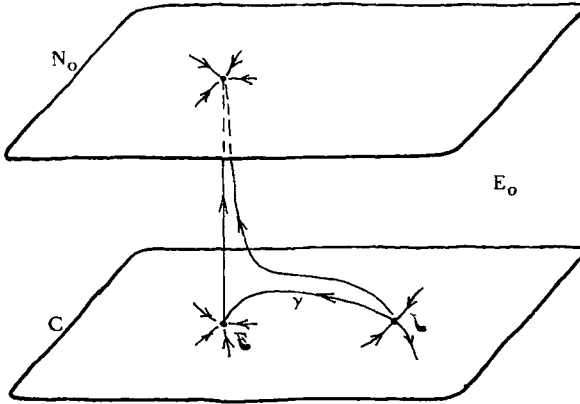


Fig. 6. An orbit off C in the unstable manifold of the Lagrange point asymptotically approaches the Euler point in N_0 .

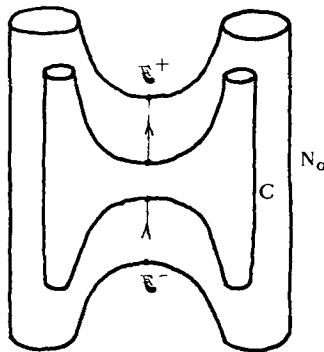


Fig. 7.

The reason is that the homographic solution ejecting from E connects to the corresponding hyperbolic equilibrium point on N_0 , as shown in Figure 6. This last point turns out to be a sink, as we easily see.

Example 2. Consider the rectilinear 3-body problem [5]. Here we can show the existence of motions asymptotically starting and ending on a parabolic escape of the Euler type for some values of the mass parameters. The topology is similar to that of the isosceles problem (see Figure 7). The difference is that there is only one central configuration (of the Euler type). The equilibrium points on C (and on N_0) are saddles, and there are two homographic solutions.

We have to restrict ourselves to mass values such that there is a saddle-saddle connection between the two equilibrium points. From the projectability of the flow on $E_0 \cup C \cup N_0$ it is clear that the 2-dimensional unstable manifold W of E^- coincides

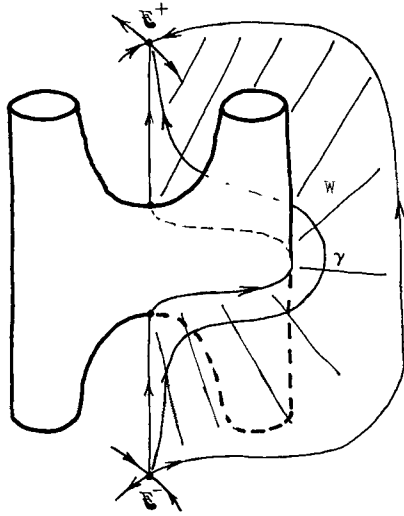


Fig. 8. Orbit γ asymptotically coming and going to parabolic escape, while passing close to triple collision.

with the stable manifold of E^+ (Figure 8). This implies the existence of an orbit γ with the desired properties.

We can also find γ , so that it passes as close as we like from triple collision (i.e., from the equilibrium points on C), if we choose it on W close enough to the homographic solutions.

3. Positive Energy Surfaces

For $h > 0$, we take again as scaling variable $\rho = I^{-1/2}$ and the change of positions $\mathbf{Q} = \rho \mathbf{q}$, but we leave the momenta unchanged, i.e., $\mathbf{P} = \mathbf{p}$. The system (1) now becomes

$$\begin{aligned} \dot{\rho} &= -\rho^2 v \\ \dot{\mathbf{Q}} &= +\rho(-v\mathbf{Q} + \mathbf{P}A^{-1}) \\ \dot{\mathbf{P}} &= \rho^2 \text{grad } U(\mathbf{Q}). \end{aligned} \quad (6)$$

with the usual normalization condition $\mathbf{Q}A\mathbf{Q}^t = 1$ and notation $v = \mathbf{P} \cdot \mathbf{Q}$. The new energy relation then becomes

$$\mathbf{P}A^{-1}\mathbf{P}^t = 2\rho U(\mathbf{Q}) + 2h \quad (7)$$

In this case there is no singularity at all when $\rho = 0$. We can still divide out the factor ρ in (6), by the time scaling

$$d\tau = \rho dt,$$

getting the following system

$$\begin{aligned}\rho' &= -\rho v \\ \mathbf{Q}' &= -v\mathbf{Q} + \mathbf{P}A^{-1} \\ \mathbf{P}' &= \rho \operatorname{grad} U(\mathbf{Q}).\end{aligned}\tag{8}$$

Notice that (8) differs from (4) in the last equation only, which in addition has now a factor ρ .

If we set $\rho = 0$ in the energy Equation (7), we get

$$\mathbf{P}A^{-1}\mathbf{P}' = 2h.\tag{9}$$

This means that in total escape the square A^{-1} norm of \mathbf{P} tends to a constant value, the *hyperbolic speed at infinity*. As before, the infinity manifold is defined by

$$N_h = \{(\rho, \mathbf{Q}, \mathbf{P}) : \rho = 0, \quad \mathbf{Q}A\mathbf{Q}' = 1, \quad \mathbf{P}A^{-1}\mathbf{P}' = 2h\}.$$

Again, N_h and the total collision manifold C defined in (5) appear as boundary components of the energy surface E_h . In the present coordinate system, this is defined as

$$E_h = \{(\rho, \mathbf{Q}, \mathbf{P}) : \rho > 0, \quad \mathbf{Q}A\mathbf{Q}' = 1, \quad \mathbf{P}A^{-1}\mathbf{P}' = 2\rho U(\mathbf{Q}) + 2h\}.\tag{10}$$

The equilibrium points of (8) on N_h are more numerous than those on C :

THEOREM 2. *If $h > 0$, the equilibrium points of the flow on N_h form a lower dimensional submanifold. The escape motions have a fixed hyperbolic speed at infinity.*

Proof. For the critical points, we are now only left with the equations $\rho = 0$, and

$$\mathbf{P}A^{-1} = v\mathbf{Q}.\tag{11}$$

Since any asymptotic approach to N_h takes place at equilibrium points, we see that, in principle, any limiting position at total escape is now permitted, but only with a fixed *hyperbolic velocity at infinity* given by (11). We saw above that its square norm is always $2h$. From (9) and (11) we see that at equilibrium points the hyperbolic speed is exactly $|v| = \sqrt{2h}$ Q.E.D.

This result is radically different from the situation on the total collision manifold, and on N_0 (Section 2). However, it reflects the fact that h takes now the place of U in energy Equation (7).

PROPOSITION. *If $h > 0$, the flow on N_h is still gradient-like with respect to v .*

Proof. Indeed, when $\rho = 0$, we get $v' = 2h - v^2 = \mathbf{Q}'A\mathbf{Q}' \geq 0$. Whenever $v' = 0$, we get $\mathbf{Q}' = 0$ and are in an equilibrium point. Q.E.D.

Therefore, $|v| \leq \sqrt{2h}$ on N_h . This is not in contradiction with the case $h = 0$, since the scaling in the momenta is different here.

4. Negative Energy Surfaces

For $h < 0$ there are zero velocity surfaces in configuration space, and escape can only occur in certain directions. In general, we will have several components of infinity manifolds, according to the problem. Clearly, escape can take place only when the potential energy has grown to produce a big enough kinetic energy.

In fact, the only way of escape to infinity of configuration space is by being close to lower order collisions, because of the structure of zero velocity surfaces. Hence, once we omit the origin (total collapse), we count the number of infinity manifold components of the energy surface $E_h, h < 0$ by the number of topological components of the lower order collisions set.

For example, in the isosceles or rectilinear 3-body problem (whose topology of configuration space is the same), we have exactly two infinity manifold components. In the general 3-body problem (spatial or planar) we have 3 components, corresponding to binary collision of the possible pairs of particles. It is clearly impossible to pass from one to the other without a total collapse.

The general situation is still far from being well understood, and it seems that the technique we give below works only for pieces of the infinity manifolds which correspond to codimension 1 subsets of the configuration space. We will illustrate this with the isosceles 3-body.

ISOSCELES PROBLEM

Consider Example 1 of Section 2, but now with $h < 0$. Referring to the masses and Jacobi coordinates of Figure 1, the energy equation can be written as follows, with $A = \text{diag} (2, 2\alpha/(2 + \alpha))$.

$$\mathbf{p}A^{-1}\mathbf{p}^t = x^{-1} + 4\alpha/\sqrt{x^2 + y^2} + 2h. \tag{12}$$

The allowed region of motion in configuration space looks like Figure 9 below. It is bounded on the right by the zero velocity curve, obtained by letting the right-hand side of (12) be equal to zero.

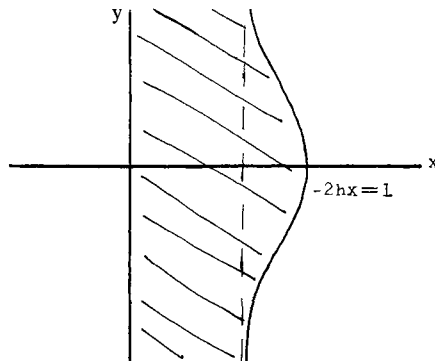


Fig. 9.

The zero velocity curve is asymptotic to the line $2hx = -1$. This gives an asymptotic bound on the possible values of x when $|y|$ is big enough. We now have two possibilities: $y > 0$ or $y < 0$, representing each of the infinity manifold components. Assume, without loss of generality, that $y > 0$.

It is then natural to make the change of variables $y = \rho^{-1} > 0$. (12) can now be written as follows

$$\mathbf{p}A^{-1}\mathbf{p}' = x^{-1} + 2h + \rho R(\rho x, 1), \quad (13)$$

where $R(x, y) = 4\alpha(x^2 + y^2)^{-1/2}$. The following flow is then obtained with no time change needed

$$\begin{aligned} \dot{\rho} &= -\rho^2(2 + \alpha)p_2/(2\alpha) \\ \dot{x} &= p_1/2 \\ 2\dot{\mathbf{p}} &= \text{grad}(1/x) + \rho^2 \text{grad} R(\rho x, 1). \end{aligned} \quad (14)$$

Notice that there are no equilibrium points, since $\text{grad}(1/x) = (-1/x^2, 0)$ is bounded away from zero for bounded x . This is the result of the total energy being negative, and can be explained as follows: since $y \rightarrow \infty$ corresponds to separation of the binary pair from the third particle with some limiting velocities, the clusters separation energy is non-negative. This implies that the inner energy of the binary is necessarily negative (see [4] for definitions of clusters of particles and partition energies). In fact, we show below that in the limit $\rho = 0$ we get bounded Kepler motions.

When $\rho = 0$, system (14) becomes particularly simple:

$$\dot{\rho} = 0, \quad 2\dot{x} = p_1, \quad 2\dot{p}_1 = -x^{-2}, \quad \dot{p}_2 = 0.$$

Elimination of p_1 and integration of the last equation gives

$$\ddot{x} = -(2x)^{-2}, \quad p_2 = \text{const.}$$

The motion has been uncoupled as a Kepler motion in the x -direction, and a trivial motion in the vertical direction. Once the binary collisions are regularized by the Levi-Civita or Sundman method, we see that the Kepler motion gives periodic orbits (negative energy), parametrized by p_2 . Rewriting the energy Equation (13) as

$$\dot{x}^2/2 - (4x)^{-1} = h/2 - (2 + \alpha)p_2^2(8\alpha)^{-1},$$

we see that the equivalent energy is

$$\bar{h}(p_2) = h - (2 + \alpha)p_2^2/(4\alpha) < 0. \quad (15)$$

In particular, the parabolic periodic orbit at infinity is easily obtained if we let $p_2 = 0$. This is a Kepler orbit with energy $\bar{h} = h$, according to (15).

The corresponding component submanifold at infinity before regularization of binary collisions is

$$N_h^+ = \{(x, \rho, p_1, p_2) : \rho = 0, \quad p_1 = 2\dot{x}, \quad \mathbf{p}A^{-1}\mathbf{p}' = 1/x + 2h\}.$$

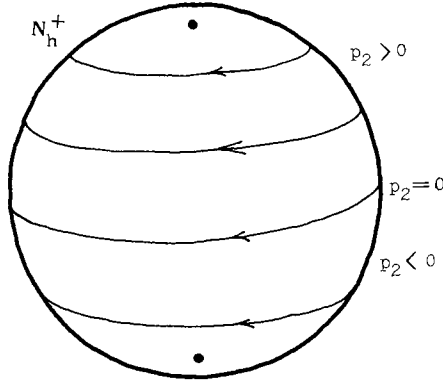


Fig. 10. Flow on one of the infinity components of the isosceles problem for $h < 0$.

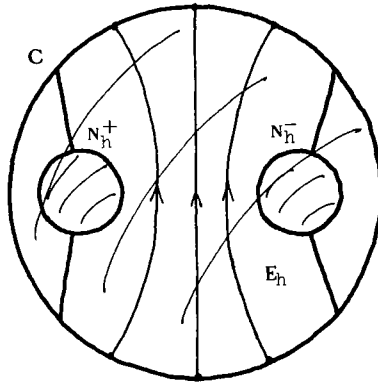


Fig. 11. Topological description of E_h and its boundary components C, N_h^+, N_h^- for $h < 0$. Four line segments connecting the outer sphere to the interior ones, are deleted.

Similarly, we can define N_h^- for the case $y < 0$. These sets are topologically S^1 -bundles over $\{x \in R : 0 < -2hx \leq 1\}$, which turns out to be an open 2-disk. After regularization, we get a sphere S^2 , where the North and South poles are deleted. We show this in Figure 10, where the parallels are Kepler orbits and the Northern Hemisphere corresponds to $p_2 > 0$, and, in particular, the North Pole corresponds to $p_2 \rightarrow \infty$. Symmetrically $p_2 < 0$ for the Southern Hemisphere. The two poles are related to hyperbolic escape with unbounded velocity.

As to the flow neighboring the boundary N_h^+ on E_h , we see from (14) that when $\rho \neq 0$ we get $\dot{p}_2 < 0$. This means that the flow spirals downward (Figure 10). Also, $p_2 \leq 0$ implies $\dot{\rho} \geq 0$, so that any asymptotic approach of the flow is forbidden in the Southern Hemisphere. If an orbit approaches the Northern Hemisphere it must always remain in the region $p_2 > 0$. By time reversal, we see that p_2 increases, and asymptotic approach for $t \rightarrow -\infty$ occurs in the Southern Hemisphere.

Finally, in Figure 11 we show topologically $E_h \cup N_h^+ \cup N_h^- \cup C$. This figure has already been described in [2], except that N_h^+, N_h^- were missing. The homographic orbits are also shown.

The same method works in the rectilinear three-body problem considered in Example 2 of Section 2. The topology turns out to be exactly the same as in Figure 11, except that, of course, there is only one homographic orbit.

5. General Homogeneous Potentials

In this section we extend our results for energy $h \geq 0$ to more general homogeneous potentials U . We consider again a system (1), where $U(q)$ is now homogeneous of degree $-d$ (see [1]).

If $h = 0$, we let again $\rho = I^{-1/2}$, $\mathbf{Q} = \rho\mathbf{q}$, but $\mathbf{P} = \rho^{-d/2}\mathbf{p}$ and $d\tau = \rho^{1+d/2} dt$. Now the new system of differential equations is almost like (4), except for the last equation, which now generalizes to

$$\mathbf{P}' = (d/2)v\mathbf{P} + \text{grad } U(\mathbf{Q}).$$

The energy relation (when we let $h = 0$) and hence N_0 , are the same as before. The equilibrium points on N_0 are central configurations of our more general potential.

For $h > 0$, we take the same scaling $\rho = I^{-1/2}$, $\mathbf{Q} = \rho\mathbf{q}$, $\mathbf{P} = \mathbf{p}$, $d\tau = \rho dt$ as in Section 3. Again this almost gives system (8), except that the last equation now reads

$$\mathbf{P}' = \rho^d \text{grad } U(\mathbf{Q}).$$

The energy relation (7) now becomes

$$\mathbf{P}A^{-1}\mathbf{P}' = 2\rho^d U(\mathbf{Q}) + 2h.$$

The manifold N_h and its flow are the same as in the Celestial Mechanics case. In particular, its equilibrium points are still defined by (11).

Note added in proof: The manifold E_n is topologically a 3-hole solid torus in Figure 3. It is just a 2-hole solid torus in Figure 11. In both cases, the 4 deleted rays correspond to collapsed binaries (with infinite speed).

References

- [1] Devaney, R. : 1980, *J. Diff. Geom.* **15**, 285–305.
- [2] Lacomba, E. A. and Losco, L. : 1980, *Bull. Am. Math. Soc.* (New Series) **3**, 710–714.
- [3] Marchal, C. and Losco, L. : 1980, *Astron. Astrophys.* **84**, 1–6.
- [4] Marchal, C. and Saari, D. G. : 1976, *J. Diff. Eq.* **20**, 150–186.
- [5] McGehee, R. : 1974, *Inventiones Math.* **27**, 191–227.
- [6] Simó, C. : 1981, in R. L. Devaney and Z. H. Nitecki (eds.), *Classical Mechanics and Dynamical Systems*, Marcel Dekker, New York, p. 203.